

Photoemission and inverse photoemission study of the electronic structure of C₆₀ fullerenes encapsulated in single-walled carbon nanotubes

H. Shiozawa,^{1,*} H. Ishii,² H. Kihara,² N. Sasaki,² S. Nakamura,² T. Yoshida,² Y. Takayama,² T. Miyahara,² S. Suzuki,² Y. Achiba,² T. Kodama,² M. Higashiguchi,³ X. Y. Chi,³ M. Nakatake,¹ K. Shimada,¹ H. Namatame,¹ M. Taniguchi,^{1,3} and H. Kataura⁴

¹Hiroshima Synchrotron Radiation Research Center, Hiroshima University, 2-313, Kagamiyama, Higashi-Hiroshima, 739-8526, Japan

²Graduate School of Science, Tokyo Metropolitan University, 1-1, Minami-Ohsawa, Hachioji, Tokyo 192-0397, Japan

³Graduate School of Science, Hiroshima University, 2-313, Kagamiyama, Higashi-Hiroshima, 739-8526, Japan

⁴Nanotechnology Research Institute, National Institute of Advanced Industrial Science and Technology, Tsukuba 305-8562, Japan

(Received 11 September 2005; revised manuscript received 16 December 2005; published 2 February 2006)

We have measured the valence-band photoemission and inverse photoemission spectra of single-walled carbon nanotubes (SWNTs) with mean radii of 0.7 and 0.64 nm encapsulating C₆₀ fullerenes (peas), so-called “peapods.” The photoemission spectrum of the C₆₀ peas in the SWNTs is obtained by subtracting the spectrum of empty SWNTs from the spectrum of the peapod. The structures in the C₆₀ pea spectra correspond well to those in the spectrum of a C₆₀ face-centered-cubic solid. No structure is observed at binding energies ranging from the Fermi level (E_F) to the onset of the highest occupied molecular orbital (HOMO) peak; the t_{1u} level of the C₆₀ peas inside the SWNT stays above E_F .

DOI: 10.1103/PhysRevB.73.075406

PACS number(s): 73.22.-f, 79.60.-i

I. INTRODUCTION

Hybrid carbon material consisting of single-walled carbon nanotubes (SWNTs) and C₆₀ fullerenes, known as peapods,^{1,2} has attracted much attention because of its nanoscale structure, which has the potential to drastically change the electronic properties of SWNTs and C₆₀ fullerenes. The electronic structures of C₆₀ peapods (C₆₀ PPDs) have been intensively studied both theoretically^{3–11} and experimentally.^{12–15} For example, using a density functional theory (DFT) calculation taking into account hybridization between the C₆₀ molecular π states and nearly free-electron (NFE) states of SWNTs, Okada *et al.*^{3,4} and Otani *et al.*⁵ pointed out that the intersection of the t_{1u} band of C₆₀ peas with the Fermi level (E_F) leads to the appearance of a multicarrier state in metallic C₆₀ PPDs. However, using a DFT calculation taking into account hybridization between C₆₀ and the SWNT unoccupied π states, Dubay and Kresse concluded that the t_{1u} band stays above E_F .⁹ Moreover, on the basis of the extended Hückel method, Rochefort stated that the band gap between the highest occupied molecular orbital (HOMO) level and t_{1u} level is decreased compared with the band gap in a C₆₀ face-centered-cubic (fcc) solid.¹⁰

Spectroscopic studies have also been performed by several groups.^{12–14} For example, Pichler *et al.* reported from an investigation of the intercalation properties of C₆₀ PPDs with Raman spectroscopy that the t_{1u} level of the C₆₀ does not lie close to E_F .¹² Using C 1s core-level excitation electron-energy-loss spectroscopy (EELS), Liu *et al.* demonstrated that the electronic and optical properties of C₆₀ peas are very similar to those of C₆₀ fcc solids.¹³ The authors concluded that the C₆₀ π states weakly hybridize with the SWNT π states.^{12,13} In contrast, Hornbaker *et al.* detected periodic spatial modification of the unoccupied π states of SWNTs corresponding to the C₆₀ array above E_F using scanning tunneling microscopy (STM), and concluded that the C₆₀ π states

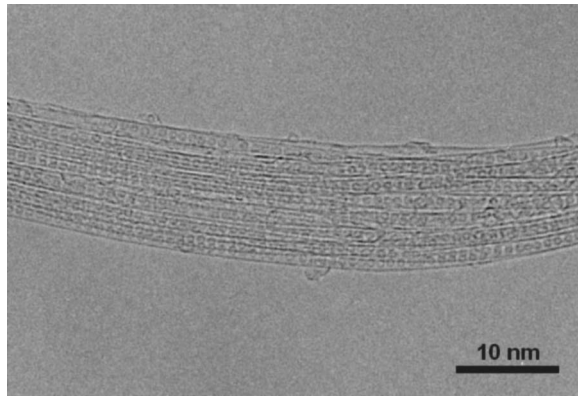
strongly hybridize with the SWNT π states.¹⁴ As mentioned above, many investigations have been performed; however, the electronic structures of C₆₀ PPDs remain a subject of controversy. It is, therefore, necessary to verify these electronic features through reliable experiments using high-purity samples.

Recent successes in the production of high-purity SWNT samples have enabled us to detect prominent peak structures in optical absorption and photoemission spectra^{16,17} due to one-dimensional van Hove singularities (VHSs), the features of which depend on the chiral angle and radius of the SWNTs.¹⁸ The purpose of this study is to investigate the electronic structure of C₆₀ PPDs by photoemission and inverse photoemission spectroscopy, which allows direct observation of the occupied and unoccupied density of states, respectively.

II. EXPERIMENTAL

The SWNT samples SWNT-A and SWNT-B were prepared using the laser ablation method and purified with H₂O₂ treatment.¹⁶ The mean radii of the SWNTs in the empty SWNT-A and SWNT-B samples were estimated to be 0.7 and 0.64 nm, respectively, through Raman spectroscopy. These values are large enough to encapsulate C₆₀ peas with a radius of 0.34 nm.^{3–6,10} The C₆₀ PPD samples C₆₀ PPD-A and C₆₀ PPD-B were synthesized by exposing the SWNT-A and the SWNT-B, respectively, to vapor phase C₆₀ in a sealed quartz tube. From x-ray diffraction analysis, we estimated the filling factor of the C₆₀ PPD-A to be 85%.¹⁹ Transmission electron microscopy (TEM) also exhibited the high-filling factor of the C₆₀ PPD-A as shown in Fig. 1.

Photoemission experiments were performed using an angle-integrated hemispherical electron energy analyzer at beamline BL-1 of the Hiroshima synchrotron radiation research center (HiSOR), Hiroshima University, and at beam-

FIG. 1. TEM image of C_{60} PPD-A sample.

line BL-11D of the Photon Factory (PF), High Energy Accelerator Research Organization. Photoemission spectra were recorded at room temperature with experimental resolutions of 35 meV at HiSOR and 50 meV at the PF. The inverse photoemission spectra were measured using a spectrometer consisting of a varied-line-spaced spherical grating and a two-dimensional position sensitive detector in Tokyo Metropolitan University.²⁰ In general, the inverse photoemission spectrum is measured with bremsstrahlung isochromat spectroscopy (BIS) mode detecting the constant photon energy (E_p) or tunable photon energy (TPE) mode using the incident electron beam with the constant energy (E_i). In this study, the spectra were measured with TPE mode using the incident electron beam of $E_i=76$ eV. The experimental resolution was 0.5 eV. Zero of the binding energy scale and the experimental resolution were calibrated with the Fermi edge of an evaporated Au film. We heated the samples at about 200 °C under an ultrahigh vacuum for several hours before each series of measurements to ensure a clean surface. Cleanliness was confirmed through the disappearance of the O $2p$ peak located at a binding energy of 6 eV.

III. RESULTS AND DISCUSSION

Figure 2 shows the photoemission spectra of the SWNT and C_{60} PPD samples measured at $h\nu=65$ eV. The photoemission spectra of the C_{60} PPD are, as a whole, similar to those of the SWNT, except for some additional peaks or shoulders in the C_{60} PPD spectra, and essentially composed of sp^2 hybrid σ and π states. The inverse photoemission spectra of the SWNT-A and C_{60} PPD-A samples are shown in the negative binding energy region in Fig. 2. The spectral shape of the SWNT-A is, as a whole, similar to that of graphite.²¹ A broad peak around -9.3 eV is mostly due to transition into the unoccupied σ^* states of the SWNTs. A prominent peak at -2.5 eV is mostly due to transition into the unoccupied π^* states of the SWNTs. The π^* and σ^* peaks in the C_{60} PPD spectrum are broader than those in the SWNT spectrum. This is due to the spectral weight coming from the C_{60} pea molecular states.

Figure 3 shows the detailed spectra of the C_{60} PPD and SWNT samples at binding energies below 1.5 eV. Three peak structures originating from the one-dimensional VHS

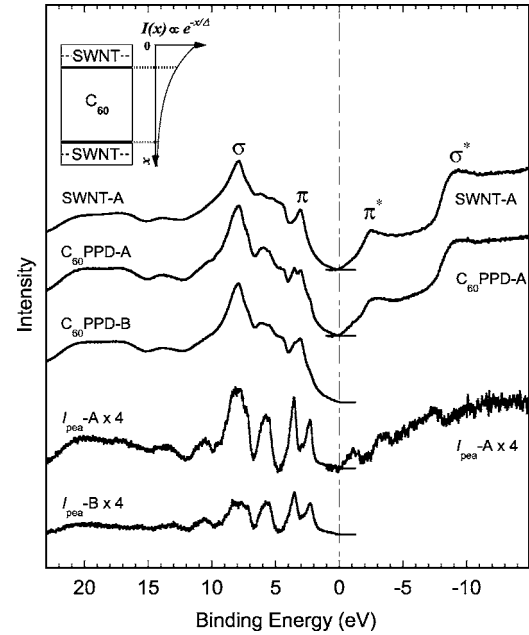


FIG. 2. Photoemission spectra of the C_{60} PPD and SWNT samples measured at HiSOR, and the C_{60} pea spectra (I_{pea}) multiplied by 4. Inverse photoemission spectra of the C_{60} PPD-A and SWNT-A samples and the C_{60} pea spectrum (I_{pea}) are plotted in the negative binding energy region. The inset shows the alternate SWNT and C_{60} layer model (left) with a photoemission intensity of $I(x) \propto \exp(-x/\Delta)$ as a function of depth from the surface x (right), where Δ represents the electron escape depth.

can be seen in all spectra. Previously, Ishii *et al.* successfully reproduced the photoemission spectrum using a tight-binding calculation taking into account the Gaussian distribution of the SWNTs radius.¹⁷ Using their procedure, we calculated the photoemission spectra of the samples. The standard de-

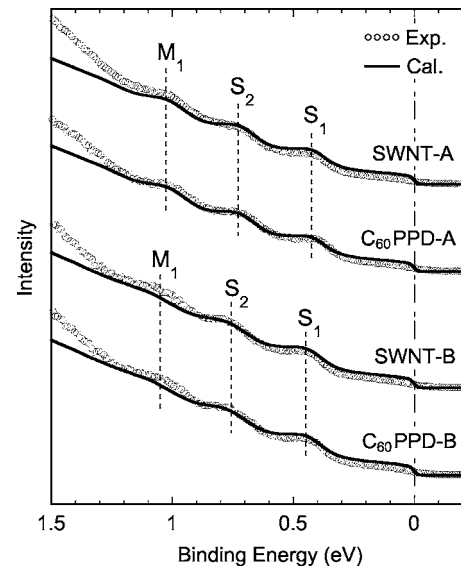


FIG. 3. Photoemission (circles) and calculated (solid line) spectra of the C_{60} PPD and SWNT samples near E_F . The S_1 and S_2 peaks and M_1 peak correspond to the structures of semiconducting and metallic SWNTs, respectively.

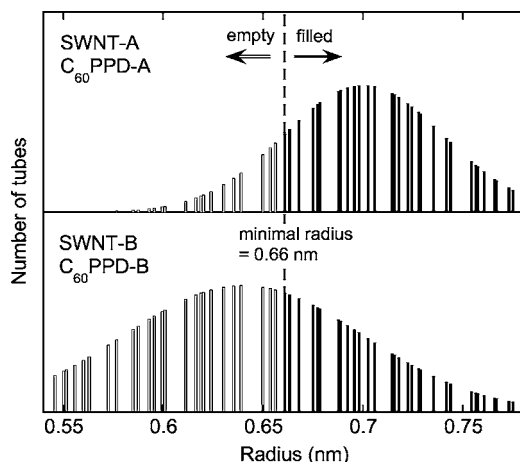


FIG. 4. Radius distribution of the SWNT and C_{60} PPD samples. The PPD samples consist of SWNTs encapsulating C_{60} (painted rectangles) and empty SWNTs (open rectangles). The minimal radius of the SWNT which can encapsulate C_{60} was estimated to be 0.66 nm.

viations of the Gaussian distribution of the SWNT radius in the empty SWNT-A and SWNT-B samples were estimated as 0.04 and 0.06 nm, respectively. The radius distributions assumed are shown in Fig. 4. Identical values were also obtained with the C_{60} PPD samples, indicating that geometrical modification of the SWNT due to inclusion of the C_{60} peas is undetectably small within the present experimental resolution. This result is consistent with the EELS result showing that the electronic properties of the SWNT and PPD are very similar to each other.¹³ Using the radius distribution shown in Fig. 4 and taking into account the filling factor of 85% for the C_{60} PPD-A sample, the minimal SWNT radius which can encapsulate C_{60} fullerenes was estimated to be 0.66 nm. This value is in good agreement with the theoretical value of 0.64 nm predicted by Okada *et al.*³ Taking into account the minimal radius of 0.66 nm, the filling factor for the C_{60} PPD-B sample was estimated to be 40%.

The partial density of states of the C_{60} peas inside the SWNT was obtained by subtracting the empty SWNT spectrum from the C_{60} PPD spectrum as follows: In a C_{60} PPD composed of a SWNT with a radius of 0.7 nm and C_{60} peas, the ratio of the number of carbon atoms included in a unit length in the C_{60} peas to that in the SWNT is about 0.39. Because of a short photoelectron mean free path at $h\nu=65$ eV, $\Delta\sim 0.5$ nm, the photoemission signal from carbon atoms in the C_{60} peas inside the SWNT is more reduced than that from carbon atoms in the SWNT. To approximately estimate the ratio of the photoemission signal from the C_{60} peas to that from the SWNT, we assumed that the SWNT and C_{60} were alternately layered from the sample surface ($x=0$) as drawn in the inset of Fig. 2, in which the thicknesses of the SWNT and C_{60} layers are 0.33 and 1.03 nm, respectively, considering a π cloud thickness of ~ 0.33 nm. Using the above model, the ratio of the photoemission signal was estimated to decrease from ~ 0.39 to ~ 0.21 . Taking into account the C_{60} filling factor of 85% in the present C_{60} PPD-A sample, the C_{60} pea spectrum (I_{pea}) was extracted as follows: $(1+0.21\times 0.85) I_{\text{PPD}}-I_{\text{NT}}$, where I_{PPD} and I_{NT} represent the

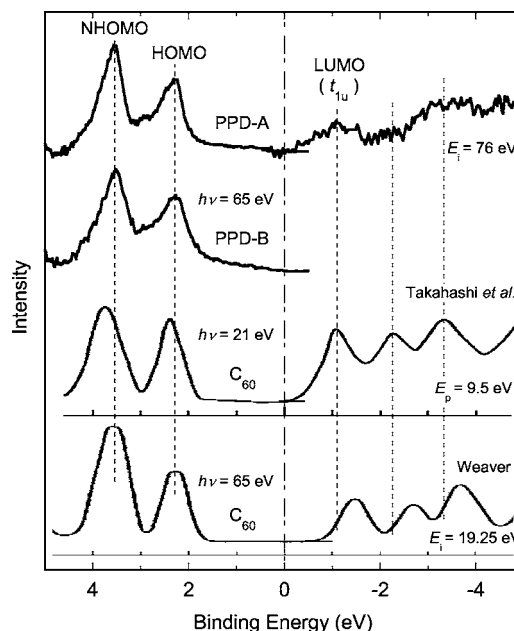


FIG. 5. Obtained C_{60} pea spectra in the binding energy region between 5 and -5 eV together with the photoemission and inverse photoemission spectra of a C_{60} solid taken from Refs. 25 and 26. In this study, the inverse photoemission spectra were measured with TPE mode using $E_i=76$ eV. The inverse photoemission spectrum in Ref. 25 was measured with BIS mode detecting $E_p=9.5$ eV and in Ref. 26 with TPE mode using $E_i=19.25$ eV.

photoemission spectra of the C_{60} PPD and SWNT, respectively, which were normalized so as to have the same integrated intensity after subtraction of respective inelastic backgrounds. In similar way, the C_{60} pea spectrum of the C_{60} PPD-B sample was extracted as $(1+0.21\times 0.40) I_{\text{PPD}}-I_{\text{NT}}$ taking into account the C_{60} filling factor of 40%. The C_{60} pea spectra are shown in Figs. 2 and 5. The overall spectral shapes are similar to those of the C_{60} solid spectra.²²⁻²⁷ The peaks in a binding energy region between 5 eV and E_F correspond mostly to the π band structures of an isolated C_{60} fullerene. The structures at binding energies above 10 eV correspond mostly to the σ band. The peaks in a binding energy region between 5 and 10 eV are a mixture of the π and σ bands.²³ The peaks at binding energies ranging from E_F to -5 eV are due to the π^* band structures.

The C_{60} pea spectra near E_F obtained for the present PPD samples are shown in Fig. 5, together with the spectra of a C_{60} fcc solid obtained by Takahashi *et al.*²⁵ and Weaver.²⁶ The peak at 2.3 eV is derived from a HOMO with h_u symmetry with fivefold degeneracy. The peak at 3.6 eV is derived from the next HOMO (NHOMO) with g_g and h_g symmetry with ninefold degeneracy. The NHOMO and HOMO peak positions are nearly equal to the respective corresponding peak positions of the C_{60} solid spectra.^{25,26} The peak located at a binding energy of -1.1 eV can be assigned to a highest occupied molecular orbital (LUMO) level with t_{1u} symmetry with threefold degeneracy of the C_{60} pea, although the LUMO peaks showed different spectral shapes depending upon the conditions of measurement.^{25,26} According to the DFT calculation of Okada *et al.*^{3,4} and Otani *et al.*,⁵ the

t_{1u} level of the C_{60} pea intersects with E_F when the SWNT radius is larger than 0.64 nm. However, as shown in Fig. 5, there is no structure in binding energies ranging from the onset of the HOMO peaks to E_F with the present PPD-A sample, which has a SWNT mean radius of 0.7 nm; the t_{1u} peak of the C_{60} peas stays above E_F . These results are consistent with the experimental results of the potassium and electrochemical doping effect and EELS,^{12,13,15} and with the prediction made by Dubay and Kresse using the DFT calculation.⁹

As mentioned above, the present photoemission and inverse photoemission data indicate that the t_{1u} level of the C_{60} peas stays above E_F even when the SWNT mean radius is larger than 0.7 nm. If electrons transfer from the SWNT to the C_{60} peas under encapsulating C_{60} fullerenes, the unoccupied t_{1u} level of the C_{60} peas can shift toward E_F . We must, therefore, consider the effect of charge transfer on the t_{1u} level of the C_{60} peas. The doping effect on the electronic structure of C_{60} fullerenes has been investigated on A_xC_{60} (A =alkali metal) solids, which exhibit a variety of interesting electronic properties ranging from insulators to high- T_C superconductors.²⁸ Regarding doped A_xC_{60} solids, when a triply degenerated t_{1u} level of C_{60} fullerenes is partially filled with doped carriers, it is well known that the Jahn-Teller effect is consequently induced.²⁸ Also, as for C_{60} PPDs, the degeneracy of the t_{1u} level of the C_{60} peas is expected to be removed, because the symmetry of the doped C_{60} cage in SWNT is lowered from the icosahedral I_h symmetry. As a result, static lattice distortion of the C_{60} cage will occur, which might lead to structural deformation of the SWNT, such as undulation of the SWNT wall. However, taking into account the fact that Peierls instability due to a lattice distortion does not occur in SWNTs,^{17,18} such a structural transformation is likely to be blocked because of the high energy cost of changing the SWNT geometry. Thus, it is probable that electron doping to the t_{1u} level of the C_{60} peas does not occur in C_{60} PPDs.

Okada *et al.*^{3,4} and Otani *et al.*⁵ proposed an energy shift of the t_{1u} level of C_{60} peas originating from hybridization between the C_{60} π states and NFE states of SWNTs; they indicated that electrons are transferred mainly from π orbitals of the SWNT to the interstitial space between the SWNT and C_{60} peas. According to their DFT calculation,³⁻⁵ a downward shift of the electronic levels of C_{60} peas occurs, while on the other hand, the occupied π band of the SWNT shifts toward E_F by about 0.1 eV. As shown in Fig. 3, however, the VHS peaks in the C_{60} PPD spectra are located at the same binding energies as their respective VHS peaks in the SWNT spectra within the experimental accuracy. This fact demonstrates that such charge transfer is negligibly small.

The NHOMO peak width in the C_{60} pea spectrum seems to be slightly narrower than that in the C_{60} solid spectrum obtained by Golden *et al.*²⁷ under similar experimental conditions, while the HOMO peak width is similar. The full width at half maximum (FWHM) of the NHOMO peak in the C_{60} pea spectrum was estimated to be 0.6–0.7 eV, which is slightly narrower than 0.8 eV in the C_{60} solid spectrum. In fcc crystal geometry, inter-fullerene electron hopping results in band dispersion of the π states, so that broad HOMO and NHOMO peaks are observed in the C_{60} photoemission

spectrum.^{23,24,29-32} According to the angle-resolved photoemission study by Gensterblum *et al.*³³ dispersion of the HOMO bands in C_{60} solids is of the order of 0.4 eV. Within a simple tight-binding model, the intrinsic band width depends, to the first order, only on intermolecular π band overlap, and is proportional to nt , where n is the number of nearest neighbor fullerenes, and t is the nearest neighbor transfer energy integral, which depends on the molecular orbital and inter-fullerene distance d . In an ideal C_{60} chain, n is reduced from 12 in the C_{60} fcc solid to 2. The distance d between adjacent C_{60} peas was estimated to be about 0.95 nm by electron and x-ray diffraction measurements, shrinking from $d=1.0$ nm for the C_{60} fcc solid.³⁴ Using the empirical relationship $t \propto d^{-2.7}$,³² the inherent π band width of an ideal one-dimensional C_{60} chain is reduced by a factor of 0.8 from that in the C_{60} fcc solid; dispersion of the HOMO bands of the C_{60} chain is expected to be of the order of 0.08 eV, which is much smaller than the observed width.

Hornbaker *et al.* discussed the degree of electron hopping between adjacent C_{60} peas, and between a C_{60} pea and SWNT.¹⁴ From a semiempirical calculation with a strong coupling energy of 1.25 eV between SWNT π states and the t_{1u} states of the C_{60} pea, they concluded that electron hopping between adjacent C_{60} peas is not as dominant as indirect electron hopping between C_{60} peas through the SWNT. If their conclusion is applied to the whole π bands of the C_{60} peas, the HOMO and NHOMO peaks in the C_{60} pea spectrum should be broader than those in the C_{60} solid spectrum, which is contrary to our result. On the other hand, according to the DFT calculation by Lu *et al.*⁶ the electron transfer energy between the SWNT and C_{60} π states is much weaker, ~ 0.1 eV. This implies that the π derived peak width in the C_{60} pea spectrum should be narrower than those in the C_{60} solid spectrum. The observed narrowing of the NHOMO width is qualitatively consistent with the prediction of the DFT calculation.³⁻¹⁰

In summary, we successfully observed C_{60} -derived structures in the valence-band photoemission and inverse photoemission spectra of C_{60} PPDs. The C_{60} pea spectra exhibited structures similar to those in the C_{60} solid spectra. We did not find evidence showing a relative energy shift of the electronic levels between C_{60} and SWNT in the C_{60} PPD. This fact indicates that unusual electronic properties, such as the theoretically predicted multicarrier character, cannot be expected with encapsulation of C_{60} fullerenes.

ACKNOWLEDGMENTS

This study was performed under the Cooperative Research Program of HiSOR, Hiroshima Synchrotron Radiation Center, Hiroshima University (04A8), and with the approval of the Photon Factory Advisory Committee (2004G199). This study was supported by a Grant-in-Aid for Scientific Research from the Ministry of Education, Culture, Sports, Science and Technology, Japan. This work was in part supported by Industrial Technology Research Grant Program in '03 from New Energy and Industrial Technology Development Organization (NEDO) of Japan.

- *Present address: Leibniz Institute for Solid State and Materials Research Dresden, D-01171 Dresden, Germany.
- ¹B. W. Smith, M. Monthieux, and D. E. Luzzi, *Nature (London)* **396**, 323 (1998).
- ²H. Kataura, Y. Maniwa, T. Kodama, K. Kikuchi, K. Hirahara, K. Suenaga, S. Iijima, S. Suzuki, Y. Achiba, and W. Krätschmer, *Synth. Met.* **121**, 1195 (2001).
- ³S. Okada, S. Saito, and A. Oshiyama, *Phys. Rev. Lett.* **86**, 3835 (2001).
- ⁴S. Okada, M. Otani, and A. Oshiyama, *Phys. Rev. B* **67**, 205411 (2003).
- ⁵M. Otani, S. Okada, and A. Oshiyama, *Phys. Rev. B* **68**, 125424 (2003).
- ⁶J. Lu, S. Nagase, S. Zhang, and L. Peng, *Phys. Rev. B* **68**, 121402(R) (2003).
- ⁷M.-H. Du and H.-P. Cheng, *Phys. Rev. B* **68**, 113402 (2003).
- ⁸Y. Cho, S. Han, G. Kim, H. Lee, and J. Ihm, *Phys. Rev. Lett.* **90**, 106402 (2003).
- ⁹O. Dubay and G. Kresse, *Phys. Rev. B* **70**, 165424 (2004).
- ¹⁰A. Rochefort and CERCA. Groupe Nanostructures, *Phys. Rev. B* **67**, 115401 (2003).
- ¹¹C. L. Kane, E. J. Mele, A. T. Johnson, D. E. Luzzi, B. W. Smith, D. J. Hornbaker, and A. Yazdani, *Phys. Rev. B* **66**, 235423 (2002).
- ¹²T. Pichler, A. Kukovecz, H. Kuzmany, H. Kataura, and Y. Achiba, *Phys. Rev. B* **67**, 125416 (2003).
- ¹³X. Liu, T. Pichler, M. Knupfer, M. S. Golden, J. Fink, H. Kataura, Y. Achiba, K. Hirahara, and S. Iijima, *Phys. Rev. B* **65**, 045419 (2002).
- ¹⁴D. J. Hornbaker, S.-J. Kahng, S. Misra, B. W. Smith, A. T. Johnson, E. J. Mele, D. E. Luzzi, and A. Yazdani, *Science* **295**, 828 (2002).
- ¹⁵L. Kavan, L. Dunsch, and H. Kataura, *Chem. Phys. Lett.* **361**, 79 (2002).
- ¹⁶H. Kataura, Y. Kumazawa, Y. Maniwa, I. Umezū, S. Suzuki, Y. Ohtsuka, and Y. Achiba, *Synth. Met.* **103**, 2555 (1999).
- ¹⁷H. Ishii, H. Kataura, H. Shiozawa, H. Yoshioka, H. Otsubo, Y. Takayama, T. Miyahara, S. Suzuki, Y. Achiba, M. Nakatake, T. Narimura, M. Higashiguchi, K. Shimada, H. Namatame, and M. Taniguchi, *Nature (London)* **426**, 540 (2003).
- ¹⁸R. Saito, G. Dresselhaus, and M. S. Dresselhaus, *Physical Properties of Carbon Nanotubes*, (Imperial College Press, Imperial College, London, 1998).
- ¹⁹H. Kataura, Y. Maniwa, M. Abe, A. Fujiwara, T. Kodama, K. Kikuchi, H. Imahori, Y. Misaki, S. Suzuki, and Y. Achiba, *Appl. Phys. A* **74**, 349 (2002).
- ²⁰Y. Takayama, M. Shinoda, K. Obu, C. Lee, H. Shiozawa, M. Hirose, H. Ishii, T. Miyahara, and J. Okamoto, *J. Phys. Soc. Jpn.* **71**, 340 (2002).
- ²¹Th. Fauster, F. J. Himpsel, J. E. Fischer, and E. W. Plummer, *Phys. Rev. Lett.* **51**, 430 (1983).
- ²²J. H. Weaver, J. L. Martins, T. Komeda, Y. Chen, T. R. Ohno, G. H. Kroll, N. Troullier, R. E. Haufler, and R. E. Smalley, *Phys. Rev. Lett.* **66**, 1741 (1991).
- ²³José Luís Martins, N. Troullier, and J. H. Weaver, *Chem. Phys. Lett.* **184**, 423 (1991).
- ²⁴N. Troullier and J. L. Martins, *Phys. Rev. B* **46**, 1754 (1992).
- ²⁵T. Takahashi, S. Suzuki, T. Morikawa, H. Katayama-Yoshida, S. Hasegawa, H. Inokuchi, K. Seki, K. Kikuchi, S. Suzuki, K. Ike-moto, and Y. Achiba, *Phys. Rev. Lett.* **68**, 1232 (1992).
- ²⁶J. H. Weaver, *J. Phys. Chem. Solids* **53**, 1433 (1992).
- ²⁷M. S. Golden, M. Knupfer, J. Fink, J. F. Armbruster, T. R. Cummins, H. A. Romberg, M. Roth, M. Sing, M. Schmidt, and E. Sohmen, *J. Phys.: Condens. Matter* **7**, 8219 (1995).
- ²⁸C. C. Chancey and M. C. M. O'Brien, *The Jahn-Teller Effect in C₆₀ and Other Icosahedral Complexes* (Princeton University Press, Princeton, New Jersey, 1997).
- ²⁹W. Y. Ching, Ming-Zhu Huang, Yong-Nian Xu, W. G. Harter, and F. T. Chan, *Phys. Rev. Lett.* **67**, 2045 (1991).
- ³⁰S. Saito and A. Oshiyama, *Phys. Rev. Lett.* **66**, 2637 (1991).
- ³¹A. Oshiyama, S. Saito, N. Hamada, and Y. Miyamoto, *J. Phys. Chem. Solids* **53**, 1457 (1992).
- ³²M. Schlüter, M. Lannoo, M. Needels, G. A. Baraff, and D. Tománek, *J. Phys. Chem. Solids* **53**, 1473 (1992).
- ³³G. Gensterblum, J.-J. Pireaux, P. A. Thiry, R. Caudano, T. Buslaps, R. L. Johnson, G. Le Lay, V. Aristov, R. Günther, A. Taleb-Ibrahimi, G. Indlekofer, and Y. Petroff, *Phys. Rev. B* **48**, R14756 (1993).
- ³⁴Y. Maniwa, H. Kataura, M. Abe, A. Fujiwara, R. Fujiwara, H. Kira, H. Tou, S. Suzuki, Y. Achiba, E. Nishibori, M. Takata, M. Sakata, and H. Suematsu, *J. Phys. Soc. Jpn.* **72**, 45 (2003).